

Depth-targeted intracortical microstroke by two-photon photothrombosis in rodent brain

Masahiro Fukuda^{a,b,*}, Takayoshi Matsumura^{c,d}, Toshio Suda^{a,d} and Hajime Hirase^{e,*}

^aKumamoto University, International Research Center for Medical Sciences, Kumamoto, Japan

^bDuke-NUS Medical School, Signature Program in Neuroscience and Behavioral Disorders, Singapore

^cJichi Medical University, Division of Inflammation Research, Center for Molecular Medicine, Tochigi, Japan

^dNational University of Singapore, Cancer Science Institute of Singapore, Singapore

^eUniversity of Copenhagen, Center for Translational Neuromedicine, Faculty of Health and Life Sciences, Copenhagen, Denmark

Abstract

Significance: Photothrombosis is a widely used model of ischemic stroke in rodent experiments. In the photothrombosis model, the photosensitizer rose bengal (RB) is systemically introduced into the blood stream and activated by green light to induce aggregation of platelets that eventually cause vessel occlusion. Since the activation of RB is a one-photon phenomenon and the molecules in the illuminated area (light path) are subject to excitation, targeting of thrombosis is unspecific, especially in the depth dimension. We developed a photothrombosis protocol that can target a single vessel in the cortical parenchyma by two-photon excitation.

Aim: We aim to induce a thrombotic stroke in the cortical parenchyma by two-photon activation of RB to confine photothrombosis within a vessel of a target depth.

Approach: FITC-dextran is injected into the blood stream to visualize the cerebral blood flow in anesthetized adult mice with a cranial window. After a target vessel is chosen by two-photon imaging (950 nm), RB is injected into the blood stream. The scanning wavelength is changed to 720 nm, and photothrombosis is induced by scanning the target vessel.

Results: Two-photon depth-targeted single-vessel photothrombosis was achieved with a success rate of $84.9\% \pm 1.7\%$ and an irradiation duration of <80 s. Attempts without RB (i.e., only with FITC) did not result in photothrombosis at the excitation wavelength of 720 nm.

Conclusions: We described a protocol that achieves depth-targeted single-vessel photothrombosis by two-photon excitation. Simultaneous imaging of blood flow in the targeted vessel using FITC dextran enabled the confirmation of vessel occlusion and prevention of excess irradiation that possibly induces unintended photodamage.

© The Authors. Published by SPIE under a Creative Commons Attribution 4.0 International License. Distribution or reproduction of this work in whole or in part requires full attribution of the original publication, including its DOI. [DOI: [10.1117/1.NPh.9.2.021910](https://doi.org/10.1117/1.NPh.9.2.021910)]

Keywords: photothrombosis; multiphoton; mice; stroke; ischemia; cortex.

Paper 21060SSR received Oct. 31, 2021; accepted for publication Feb. 24, 2022; published online Mar. 16, 2022.

1 Introduction

Ischemic strokes occur at various levels of cerebral circulation ranging from massive middle cerebral artery occlusion to transient ministrokes that occur at single arterioles. Ischemia at the

*Address all correspondence to Masahiro Fukuda, mfukuda-tyk@umin.ac.jp; Hajime Hirase, hirase@sund.ku.dk

stroked sites causes neuronal death or irreversible damage that forms an infarct due to the lack of oxygen and energy substrates. Silent strokes typically occur in small arterioles and cause small-sized infarcts, resulting in little expressive symptoms. These so-called microstrokes occur in the cerebral parenchyma and remain undetected until multiple occurrences of microstrokes over a period integrate to develop into motor and/or cognitive deficits.¹

Several models have been proposed to generate local embolic or thrombotic stroke in experimental animals.^{2–4} For instance, hundreds of microspheres of diameter 20 to 50 μm have been perfused into the upstream of cerebral circulation,⁵ e.g., the internal carotid artery, to induce embolic ischemic stroke in the downstream arterioles. Microsphere infusion imposes a fair amount of surgical burdens and inherently forms infarcts in multiple places. Since the locations of infarcts are somewhat arbitrary and sometimes ectopic, this method is not optimal for observing the impact of single-vessel occlusion by microscopic *in vivo* imaging.

Induction of thrombosis by optic means, photothrombosis,⁶ has been widely utilized by the stroke research community owing to the technique's reproducibility and flexible target region selection. Photothrombosis is performed by introducing the photosensitizer rose bengal (RB) into the blood and exciting it by green light in the targeted area of the brain surface. RB excitation produces reactive oxygen species (ROS), which damages epithelial cells and promotes aggregation of platelet on the vessel wall that eventually occludes the vessel. Photothrombosis has the advantage of target area selection over other methods as the target region can be specified by guiding the excitation light illumination spot (for an example, Ref. 7). However, due to the nature of one-photon reaction, photothrombosis is not suited for targeting specific vessels inside the brain tissue because the superficial vessels including capillaries are also subjected to photothrombosis with even higher intensity light. Furthermore, excess exposure of high-intensity excitation light on the mouse cerebral cortex can penetrate into deeper structures, such as the hippocampus and striatum, and occlude off-target areas, making the interpretation of subsequent outcome unclear. Moreover, spot illumination of the thrombotic target area does not distinguish between arteries and veins.

Two-photon microscopy has been utilized widely in bioimaging due to its superior depth-penetration in the tissue and focus-specific fluorescence excitation.⁸ Taking advantage of this feature, multiphoton photothrombosis has been reported very recently by a group that employed fix-point irradiation.⁹ Here we introduce an alternative technique for depth-targeted photothrombosis (DTPT) that can readily be used on a standard two-photon microscope equipped with a resonant scanner. Using this method, we demonstrate photothrombosis in a single vessel or a group of vessels at a targeted depth of up to 300 μm . Remarkably, we show that photothrombosis can be induced at the cortical depth of 240 to 300 μm without unwanted occlusions above and below the target. These features are favorable for prospective microstroke research since inducing occlusion in individual targeted vessels in the brain parenchyma is considered to mimic silent stroke.

2 Materials and Methods

2.1 Subjects and Surgery

Adult C57BL/6 mice (2 to 6 months old, 20 to 30 g) of either sex were used. Mice were deeply anesthetized with isoflurane (5% for induction, 1.5% for maintenance). A craniotomy of ~ 3 mm diameter was performed above the somatosensory cortex while the dura was left intact. Thereafter, a 3-mm diameter glass coverslip (No. 0; Matsunami, Japan) was placed and fixed with dental cement. A metallic head frame that fits to a MAG-3 head-stager holder (Narishige, Japan) was attached to the skull, and the remaining exposed skull was covered with dental cement.

The procedures involving animal care, surgery, and sample preparation were approved by the Danish Animal Experiments Inspectorate and the Animal Care and Use committee of Kumamoto University, Kumamoto, Japan. The animal study was overseen by the University of Copenhagen Institutional Animal Care and Use Committee.

2.2 *In Vivo Two-Photon Depth-Targeted Photothrombosis*

Two-photon imaging and DTPT was performed in anesthetized mice, using a Bergamo scope (Thorlabs, NJ, USA) equipped with a resonant scanner (8 kHz), a piezo Z drive, a 25×1.1 NA water immersion lens (CFI75 Apochromat 25XC W 1300; Nikon, Japan), and a Mai Tai eHP DeepSee laser (Spectra-Physics, CA, USA). Emission light was separated by a dichroic mirror (562 nm; Chroma, VT, USA) with bandpass filters 525/50 and 607/70 nm (both from Chroma) for the green and red channels, respectively. The microscope was operated using the ThorImage LS software version 4.0. Laser power at 950 and 720 nm was measured using a laser power meter (Fieldmate and PM10, Coherent, CA) before experiments every time.

DTPT was carried out as follows. First, to maximize the excitation efficiency, we adjusted the head-stage mount angle so that the craniotomy plane became parallel to the objective lens plane using the goniometer incorporated into the MAG-3 head-stage holder.¹⁰ Second, 300 μ L of FITC-150k dextran (concentration: 20 mg/mL, Sigma-Aldrich, MO, USA) was injected intravenously (i.v.) via the retro-orbital route to label blood vessels. After identifying the target blood vessel using 950 nm excitation light, 100 μ L of the photosensitizer RB (Sigma-Aldrich, MO, USA) was injected (i.v., RB concentration: 20 mg/mL in phosphate buffered saline)¹¹ via a catheter placed in the tail vein. For multiple occlusion experiments, RB was injected every 20 min to maintain the RB concentration in the blood (up to three times). For targeting a single blood vessel at 240 to 300 μ m, RB was injected only once.

The excitation light wavelength was then changed to 720 nm, and the focal depth was readjusted to the target vessel's lumen using the least laser power possible (2.9 mW). Next, the scanned area was restricted by increasing the digital magnification to include only the targeted vessel. To start photothrombosis, the laser intensity at the exit of the objective lens was set to the necessary amount (31 mW for multiple occlusion experiments at 30 to 50 μ m, 63 mW for targeting 240 μ m, and 300 mW for targeting 300 μ m). The selected area was subsequently scanned at a high frame rate (30 to 60 Hz, depending on the scanned area) while monitoring acquired images in real time. If equipped, the far-red detection channel should be switched off to protect PMT. Scanning was terminated when blood clots were formed.

2.3 *Statistics*

Comparisons of two sample means were assessed by *t*-test. Error bars of bar graphs represent the standard error of the mean. Box plots indicate the medians and 25th and 75th percentiles of the sample data. The whiskers of the box plots represent the shorter of the data range or the outlier limit. The outlier limits are defined as $q3 + 1.5 \times (q3 - q1)$ and $q1 - 1.5 \times (q3 - q1)$, where $q1$ and $q3$ are the 25th and 75th percentiles of the sample data.

3 Results

3.1 *Repetitive Fast Scans in the Lumen Induces Two-Photon Photothrombosis*

To undertake the induction of photothrombosis by an ultrashort pulse infrared laser, we followed a recent paper that reported an enhanced multiphoton excitation of RB for wavelengths <750 nm.¹² First, we visualized the cerebral vasculature by labeling the serum with FITC-dextran via retro-orbital i.v. injection and imaging through the cranial widow by a two-photon microscope in an anesthetized mouse [Fig. 1(a)]. A wavelength of 950 nm was used to excite FITC. Cerebral arterioles were identified by tracking the downstream of a descending blood flow in the penetrating arteries. A vessel of diameter 4 to 20 μ m was chosen as a target and placed at the middle of the view field by adjusting the microscope stage. In selecting a target vessel, locations with large vessels lying above them were avoided. The scanned area was restricted to the target vessel by zooming into the vessel [Fig. 1(b)]. After injecting RB i.v. via a catheter placed in the tail vein, the wavelength was changed to 720 nm and the scanned depth (the Z axis focus) was readjusted to scan inside the lumen with a minimum laser intensity (2.9 mW) with a frame rate at 30 or 60 Hz. After setting the target, the laser power was set to 31 mW (at the exit of the

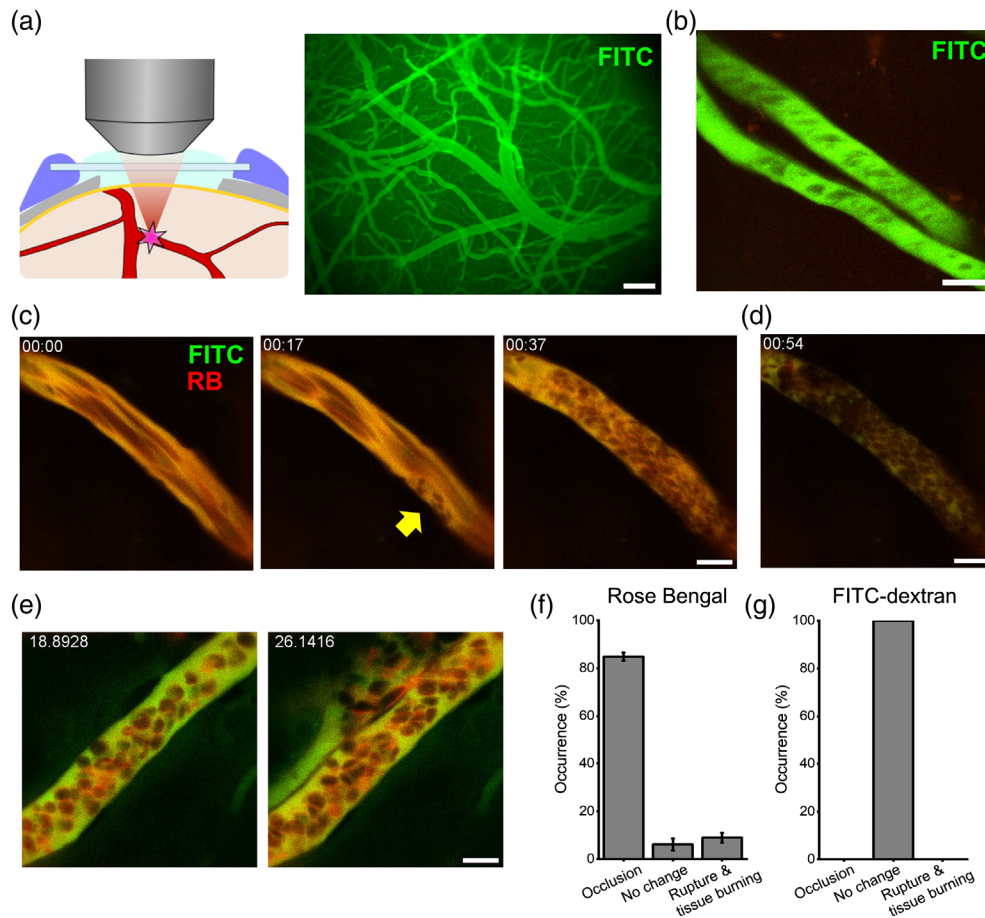


Fig. 1 *In vivo* two-photon DTPT: (a) schematic illustration of DTPT. After visualization of blood vessels with FITC-dextran, a blood vessel containing RB is targeted by two-photon excitation. (b) Blood vessels to be targeted were chosen using FITC-dextran fluorescence. (c) Following RB injection, the excitation wavelength was switched to 720 nm. Imaging of the targeted blood vessel with 720 nm wavelength was performed until coagulation was formed. (d) Completion of occlusion could be distinguished by photobleaching of RB and FITC. (e) In a small number of cases, blood vessel rupture or tissue burning was observed. (f) The success rate of DTPT was $84.9\% \pm 1.7\%$, whereas $6.1\% \pm 2.5\%$ of the cases were not occluded (no change) and $9.0\% \pm 2.1\%$ of the cases had tissue burning/rupture (occlusion: 84/99, no change: 6/99, tissue burning/rupture 9/99 vessels, 4 mice). (g) Controls with FITC-150k dextran only did not show occlusion or tissue burning/rupture in 150 s (103 blood vessels, 3 mice). Scale bars: (a) 200 μm and (b)–(e): 10 μm . Occlusion of a single cortical vessel by DTPT. Scale bar 10 μm . ([Video 1](https://doi.org/10.1117/1.NPh.9.2.021910.1), MP4, 7 MB [URL: <https://doi.org/10.1117/1.NPh.9.2.021910.1>]).

objective lens). The PMT voltage and amplifier gain was set to low values to allow for simultaneous photothrombosis and vessel blood flow monitoring.

The blood flow of the subjected vessel was recognized from the suboptimal fluorescence of RB and FITC as acquired images are updated on the screen [Fig. 1(c), left]. Initially, platelets started to attach to the blood vessel wall [Fig. 1(c), middle]. Thereafter, platelets and red blood cells (RBCs) made a clot, and the blood flow was gradually compromised [Fig. 1(c), right; [Video 1](#)]. Occlusion of the vessel was observed by the appearance of stalled platelets and RBCs in the image. In addition, the blood-contained dyes quickly became bleached and after complete occlusion, which can be used as the sign of occlusion [Fig 1(d)]. Occlusion was induced with 720 nm irradiation of duration shorter than 80 s in the majority of cases [Fig. 1(f), 84/99 vessels, 4 mice], though we have observed failure of occlusion or rupture/tissue burning in a small number of attempts [Fig. 1(f)]. In contrast, the FITC-only control displayed neither occlusion nor attachment of platelets to the vessel walls even when they were irradiated for up to 150 s [Fig. 1(g)].

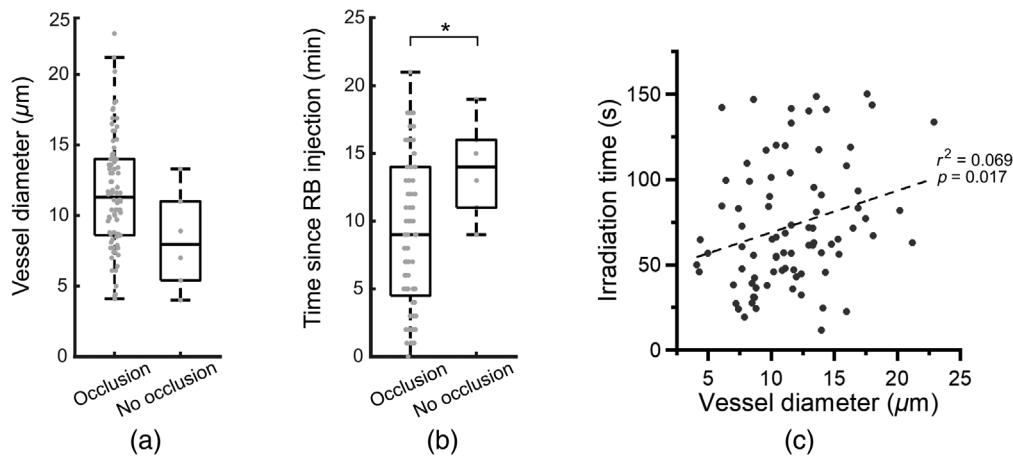


Fig. 2 Parameters for successful DTPT: (a) distribution of vessel diameter for successfully occluded vessels versus not occluded vessels. (b) Distribution of time since RB injection for successfully occluded vessels versus not occluded vessels. $*P < 0.05$. (c) Scatter plot showing the relationship between irradiation time and vessel diameter for successfully occluded vessels.

We did not find that the diameter of blood vessels affected the success of occlusion formation (occlusion: $11.58 \pm 0.43 \mu\text{m}$ ($n = 84$), no change: $8.27 \pm 1.57 \mu\text{m}$ ($n = 6$), $P = 0.069$) [Fig. 2(a)]. We find that the success rate of occlusion formation by DTPT is affected by the time since the RB injection. The unsuccessful attempts occurred when significantly longer time passed after the RB injection than typical successful attempts [successful occlusion: $9.0 \pm 0.6 \text{ min}$ ($n = 84$), no occlusion: $13.8 \pm 1.6 \text{ min}$ ($n = 6$) since the RB injection. $P = 0.019$] [Fig. 2(b)]. These results together with the FITC-only control [Fig. 1(g)] indicate that the concentration of RB inside the blood vessel is crucial for DTPT and 720-nm excitation laser reliably excites RB, most likely due to the relatively high excretion of blood RB to bile.¹³ We calculated the correlation between irradiation time and vessel diameter for successfully occluded vessels and found that they are only weakly correlated ($r^2 = 0.069$, $p = 0.017$).

3.2 DTPT Occlusion is Confined to the Targeted Vessels

The DTPT attempts that we have described thus far have been done in target planes 30 to 50 μm from the pial surface; next we perform DTPT targeting single blood vessels ($\varphi = 6.3$ to 7.0 μm) located at the depths of 240 and 300 μm . In our attempts, one vessel per animal was subjected to DTPT. For the depth of 300 μm , we used the laser power 300 mW for the 720-nm irradiation in a mouse. Accordingly, the blood clot was formed within 40 s [Figs. 3(a) and 3(b), Video 2]. The clot was clearly visible with 950 nm excitation [Fig. 3(c), arrow]. In two mice, we performed DTPT with 63 mW irradiation at depth 240 μm . Targeted vessels were successfully occluded by ~ 90 -s irradiation (Fig. S1 in the Supplementary Material). Together, all three attempts of deep-vessel DTPT were successful.

The utility of DTPT becomes powerful when off-focus vessels are not occluded. To ensure that photothrombosis was confined to the targeted vessel, we took volumetric images and examined whether there are any blood clots in the capillaries 100, 200, and 300 μm above and 100 μm below the target plane shortly after DTPT (within 5 min) at a wavelength of 950 nm. As shown in a representative image in the result, we saw no obvious clots in the off-target planes [Fig. 3(d) and Videos 3, 4, and 5]. To examine the effect of selective occlusion, we observed the area 3 days later. We found that the peripheral blood vessels of the targeted plane were also occluded, and extravasation of FITC around the occluded blood vessels was discernible [Fig. 3(e)].

4 Discussion

Photothrombosis has been studied for over three decades⁶ and remains widely used for targeted induction of ischemic stroke owing to its superior reproducibility. Despite the widespread utility,

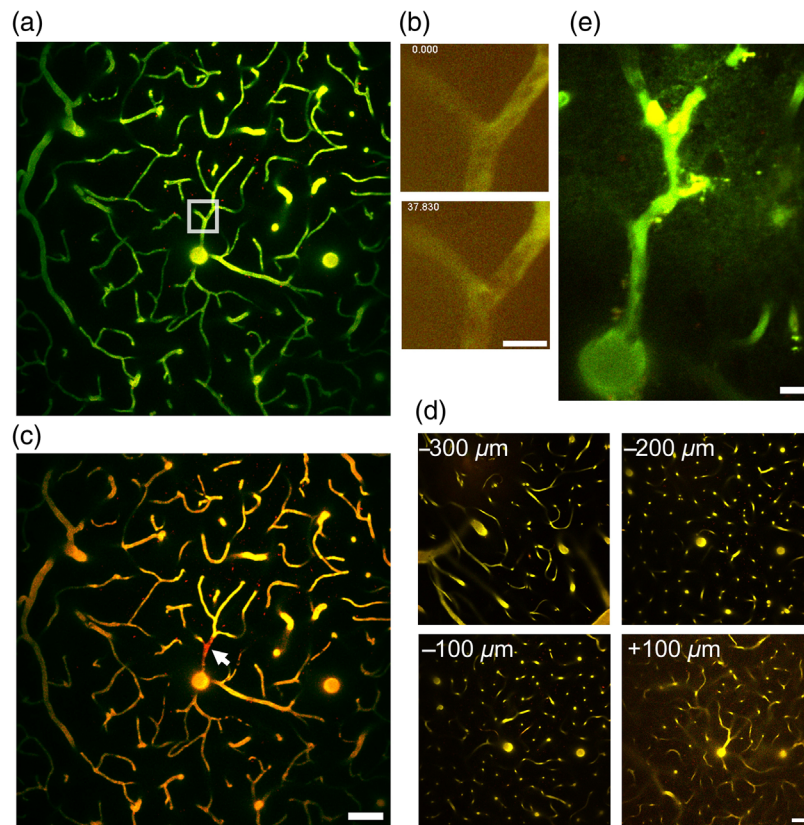


Fig. 3 Off-target effect of DTPT is negligible: (a) the blood vessel located at $300\ \mu\text{m}$ from the pia was targeted. (b) Occlusion was formed in 40 s using 300-mW 720-nm excitation laser. (c) After DTPT, the excitation was set to 950 nm, and coagulation was visualized. (d) Even using 300 mW excitation for DTPT, there was no occlusion/coagulation in areas 300, 200, 100 μm above and 100 μm below the target. (e) Extravasation of FITC-150k dextran and occlusion of peripheral blood vessels were observed three days after DTPT. Scale bars: (a), (c), (d) 50 μm and (b), (e) 10 μm . Occlusion of the vessel corresponding to (b). Scale bar 10 μm . (Video 2, MP4, 5 MB [URL: <https://doi.org/10.1117/1.NPh.9.2.021910.2>]). Depth stack of the cortical vasculature around the DTPT target site corresponding to this figure (Video 3, MP4, 12 MB [URL: <https://doi.org/10.1117/1.NPh.9.2.021910.3>]) and Fig. S1 in the Supplementary Material (upper panel, Video 4, MP4, 4 MB [URL: <https://doi.org/10.1117/1.NPh.9.2.021910.4>]) and (lower panel, Video 5, MP4, 5 MB [URL: <https://doi.org/10.1117/1.NPh.9.2.021910.5>]). Scale bar 50 μm .

photothrombosis has not been utilized for induction of microstrokes targeted specifically at a depth of the cerebral cortex until very recently. This is because conventional photothrombosis relies on one-photon excitation of RB: ROS is produced wherever the green photon hits RB; hence the formation of thrombosis is biased toward superficial vessels. On the other hand, multiphoton excitation occurs only at the focal spot, avoiding the production of ROS production outside the focal plane, and thereby enables depth-specific targeting. Indeed, Delafontaine-Martel et al. demonstrated that multiphoton occlusion is feasible by two-photon or three-photon excitation. In their study, two-photon photothrombosis was achievable in depths up to 200 μm from the pial surface, and significantly longer irradiation time (up to 300 s) was needed with an excitation wavelength of 1000 nm.⁹ In the current work, we further confirm that two-photon photothrombosis is feasible in the mouse brain. Notably, we find that <80-s irradiation is sufficient for inducing microvessel occlusion at a success rate >80% for vessels located in depths 30 to 50 μm . This accelerated two-photon photothrombosis was possible with a significantly shorter wavelength of 720 nm in the RB-injected mice but not in the FITC control mice.

The one-photon absorption spectrum of RB has a broad peak at around 560 nm, and a green light of range 530 to 580 nm is typically used for RB activation. Recently, Campaign and Knox¹² measured the two-photon excitation spectrum of RB. According to this study, the two-photon-excited fluorescence increased by approximately threefold as the excitation wavelength shifts

from 780 to 720 nm. Although the fluorescence emission does not necessarily correlate to ROS production, the demonstration of elevated molecule excitability at 720 nm prompts a future study to characterize ROS production around this wavelength. It is noteworthy that we could not observe discernible off-target photothrombosis even after targeting 240 to 300 μm with high laser power [Fig. 3(d); associated Videos 3, 4, and 5; and Fig. S1 in the [Supplementary Material](#)], indicative of focal spot-specific multiphoton excitation of RB with this wavelength. Another methodological point that we consider important for the induction of efficient photothrombosis is scanning the lumen of the target vessel and avoiding irradiating vessel walls (endothelial cells) as much as possible. This procedure, combined with simultaneous irradiation and imaging, is designed to ensure excitation of RB without damaging the vessel integrity. For this matter, it is imperative to perform DTPT shortly after RB administration, so the plasma retains sufficient RB levels.

Although not attempted in this study, the shortened time of photothrombosis induction makes it likely that this method is applicable to awake mice, which eliminates confounding factors associated with anesthetics¹⁴ and hence mimics human strokes more closely. Although photothrombosis of a single small-sized vessel would not impact the cognitive ability of the subjected mouse, we demonstrate that DTPT can be performed on multiple vessels, hence enabling scalable ischemic damage. A previous study has documented formation of a single-vessel clot using a kilohertz pulsed laser of pulse energy a few orders of magnitude more intense than a typical laser used for two-photon imaging.¹⁵ However, this method requires an intricate extra optics setup to produce the high-energy pulses. Our method works on a standard two-photon microscope without any hardware modifications; hence it appeals to the need for simplicity and versatility. It would be interesting to observe acute and chronic local perfusion changes after single-vessel DTPT and compare the outcome with the published results using high-energy pulses.¹⁵ The feasibility of vasculature imaging three days after DTPT [Fig. 3(e)] is encouraging for such a study.

Single-vessel photothrombosis has been performed on surface vessels,^{16–20} but the supposed off-target effects on deeper parenchymal vessels have not been thoroughly addressed. A clever application of one-photon photothrombosis is targeting penetrating vessels,²¹ thereby partially circumventing the issue of depth-axis-wide activation of RB. DTPT offers a distinct advantage over the conventional green light-induced photothrombosis using infrared light that penetrates deeper into the parenchyma. Hence, DTPT should be an effective means to evaluate the theoretical prediction of microstroke outcomes in various microcirculation configurations.²² Future applications of the DTPT include occlusion of subcortical regions such as the hippocampus, where two-photon or three-photon imaging from the cortical surface is possible.^{10,23–25} Our preliminary attempts suggest that this is feasible, although a thorough histological investigation of the cortical areas in the passage of the infrared beam should be performed to confirm target-specific induction of thrombotic stroke.

Another future utility of DTPT is to investigate the impact of single microvessel occlusion on the surrounding neuropil activity and inflammation. Astrocytes, a major glia subtype, have been reported to elicit aberrant activities after wide field photothrombosis.^{26,27} Chronic imaging Ca^{2+} activity or morphology will be a great resource for understanding how neuropils normalizes after the mild ischemic insult or how angiogenesis possibly occurs. Of note, we have recently described that adrenergic receptor antagonism accelerates neuronal activity recovery after wide field photothrombotic stroke²⁷ or cortical spreading depression/depolarization.²⁸ It would be interesting to examine how adrenergic receptor antagonism affects the homeostasis of the extracellular environment around a singly occluded vessel in light of the adrenergic receptor-dependent glymphatic system.^{29,30}

Disclosures

The authors declare no conflicts of interest.

Acknowledgments

M. F. is supported by Japan Society for the Promotion of Science Grant-in-Aid for Scientific Research (S) (No. JP18H05284 to T. Suda) and Japan Society for the Promotion of Science

Grant-in-Aid for Challenging Research (Exploratory) (No. JP21K19514 to T. Matsumura). H. H. is supported by the Novo Nordisk Foundation (No. NNFOC0058058), Danmarks Frie Forskningsfond (No. 0134-00107B), and the Lundbeck Foundation.

Code, Data, and Materials Availability

All materials used in the current procedure are available commercially. ThorImage LS is proprietary image acquisition software for Thorlab's multiphoton microscopes.

References

1. S. E. Vermeer, W. T. Longstreth, and P. J. Koudstaal, "Silent brain infarcts: a systematic review," *Lancet. Neurol.* **6**(7), 611–619 (2007).
2. A. Durukan and T. Tatlisumak, "Acute ischemic stroke: overview of major experimental rodent models, pathophysiology, and therapy of focal cerebral ischemia," *Pharmacol. Biochem. Behav.* **87**(1), 179–197 (2007).
3. F. Fluri, M. K. Schuhmann, and C. Kleinschnitz, "Animal models of ischemic stroke and their application in clinical research," *Drug Des. Dev. Ther.* **9**, 3445–3454 (2015).
4. C. J. Sommer, "Ischemic stroke: experimental models and reality," *Acta Neuropathol.* **133**(2), 245–261 (2017).
5. M. Kudo et al., "An animal model of cerebral infarction. Homologous blood clot emboli in rats," *Stroke* **13**(4), 505–508 (1982).
6. B. D. Watson et al., "Induction of reproducible brain infarction by photochemically initiated thrombosis," *Ann. Neurol.* **17**(5), 497–504 (1985).
7. M. Balbi et al., "Targeted ischemic stroke induction and mesoscopic imaging assessment of blood flow and ischemic depolarization in awake mice," *Neurophotonics* **4**(3), 035001 (2017).
8. W. Denk, J. H. Strickler, and W. W. Webb, "Two-photon laser scanning fluorescence microscopy," *Science* **248**(4951), 73–76 (1990).
9. P. Delafontaine-Martel et al., "Multiphoton excitation of rose bengal to induce capillary photo-thrombosis," *Proc. SPIE* **11629**, 116290G (2021).
10. M. Fukuda, K. Ozawa, and H. Hirase, "Imaging living organisms," in *Imaging from Cells to Animals In Vivo*, M. M. Barroso and X. Intes, Eds., pp. 295–306, CRC Press, Boca Raton, Florida (2020).
11. T. Yardeni et al., "Retro-orbital injections in mice," *Lab Anim.* **40**(5), 155 (2011).
12. S. M. G. Campaign and W. H. Knox, "Increase in efficacy of near-infrared femtosecond micromachining in ophthalmic hydrogels with the addition of sodium fluorescein, rose bengal, and riboflavin," *Appl. Opt.* **58**(32), 8959 (2019).
13. T. Nakazima, "Experimental and clinical studies on dyes for excretory function test of liver," *Tohoku J. Exp. Med.* **56**, 87–94 (1952).
14. A. Seto et al., "Induction of ischemic stroke in awake freely moving mice reveals that isoflurane anesthesia can mask the benefits of a neuroprotection therapy," *Front. Neuroenergetics* **6**, 1 (2014).
15. N. Nishimura et al., "Targeted insult to subsurface cortical blood vessels using ultrashort laser pulses: three models of stroke," *Nat. Methods* **3**(2), 99–108 (2006).
16. T. A. Clark et al., "Artery targeted photothrombosis widens the vascular penumbra, instigates peri-infarct neovascularization and models forelimb impairments," *Sci. Rep.* **9**(1), 2323 (2019).
17. S. Sunil et al., "Awake chronic mouse model of targeted pial vessel occlusion via photothrombosis," *Neurophotonics* **7**(1), 015005 (2020).
18. Z. J. Taylor and A. Y. Shih, "Targeted occlusion of individual pial vessels of mouse cortex," *Bio-Protoc.* **3**(17), e897 (2013).
19. A. Sigler, A. Goroshkov, and T. H. Murphy, "Hardware and methodology for targeting single brain arterioles for photothrombotic stroke on an upright microscope," *J. Neurosci. Methods* **170**(1), 35–44 (2008).

20. S. M. S. Kazmi et al., “Three-dimensional mapping of oxygen tension in cortical arterioles before and after occlusion,” *Biomed. Opt. Express* **4**(7), 1061–1073 (2013).
21. A. Y. Shih et al., “The smallest stroke: occlusion of one penetrating vessel leads to infarction and a cognitive deficit,” *Nat. Neurosci.* **16**(1), 55–63 (2013).
22. F. Schmid et al., “The severity of microstrokes depends on local vascular topology and baseline perfusion,” *Elife* **10**, e60208 (2021).
23. N. G. Horton et al., “*In vivo* three-photon microscopy of subcortical structures within an intact mouse brain,” *Nat. Photonics* **7**(3), 205–209 (2013).
24. R. Kawakami et al., “Visualizing hippocampal neurons with *in vivo* two-photon microscopy using a 1030 nm picosecond pulse laser,” *Sci. Rep.* **3**, 1014 (2013).
25. L. Streich et al., “High-resolution structural and functional deep brain imaging using adaptive optics three-photon microscopy,” *Nat. Methods* **18**(10), 1253–1258 (2021).
26. S. Ding et al., “Photothrombosis ischemia stimulates a sustained astrocytic Ca^{2+} signaling *in vivo*,” *Glia* **57**(7), 767–776 (2009).
27. H. Monai et al., “Adrenergic receptor antagonism induces neuroprotection and facilitates recovery from acute ischemic stroke,” *Proc. Natl. Acad. Sci. U. S. A.* **116**(22), 11010–11019 (2019).
28. H. Monai et al., “Adrenergic inhibition facilitates normalization of extracellular potassium after cortical spreading depolarization,” *Sci. Rep.* **11**(1), 8150 (2021).
29. J. J. Iliff et al., “A paravascular pathway facilitates CSF flow through the brain parenchyma and the clearance of interstitial solutes, including amyloid β ,” *Sci. Transl. Med.* **4**(147), 147ra111 (2012).
30. L. Xie et al., “Sleep drives metabolite clearance from the adult brain,” *Science* **342**(6156), 373–377 (2013).

Masahiro Fukuda received his MD from the University of Tokyo, Tokyo, Japan. He is a post-doctoral researcher at Duke-NUS Medical School, Singapore as well as a visiting assistant professor at the International Research Center for Medical Sciences, Kumamoto University, Kumamoto, Japan. His current focus is the functional integration of iPS cells-derived human neurons in the rodent brain.

Hajime Hirase received his BSc degree and PhD from University College London, London, UK. He did postdoctoral training at Rutgers University, Newark, NJ, USA and Columbia University, New York, NY, USA. He is a professor at the Center for Translational Neuromedicine, University of Copenhagen, Copenhagen, Denmark. He has previously worked as a principal investigator at RIKEN, Wako, Japan. His current research interests include neuron–glia interactions in the rodent brain.

Biographies of the other authors are not available.